Journal of Inorganic Biochemistry 222 (2021) 111506

Contents lists available at ScienceDirect

Journal of Inorganic Biochemistry

journal homepage: www.elsevier.com/locate/jinorgbio

Sequence dependence of Pd(II)-mediated base pairing by palladacyclic nucleobase surrogates

Madhuri Hande [1], Sajal Maity [1], Tuomas Lönnberg *

Department of Chemistry, University of Turku, Vatselankatu 2, 20014 Turku, Finland

ARTICLE INFO

Keywords:
Base pair
Hybridization
Oligonucleotide
Palladium
Metallacycle
Förster resonance energy transfer

ABSTRACT

A *C*-nucleoside derivative of phenylpyridine or the respective palladacycle was incorporated at either 3′- or 5′-terminus of a short oligodeoxynucleotide. Hybridization properties of these modified oligonucleotides were studied in a fluorescence-based competition assay in addition to conventional UV melting temperature analysis and compared with those of a previously prepared analogue featuring the modified nucleoside in the middle of the sequence. With the unpalladated phenylpyridine oligonucleotides, UV melting temperature qualitatively correlated with the ability to displace a strand from a double helix in the competition assay, decreasing in the order 5′ > 3′ > middle. Corresponding results on the palladacyclic oligonucleotides were more difficult to interpret but both UV melting and competition experiments revealed a decrease in the duplex stability upon palladation in most cases. On the other hand, dependence of the UV melting temperature on the identity of the canonical nucleobase opposite to the modified nucleobase analogue was much more pronounced with the palladacyclic duplexes than with their unpalladated counterparts. Furthermore, UV melting profiles of the palladacyclic duplexes featured an additional transition at a temperature exceeding the melting temperature of the unmodified part of the duplex. Taken together, these results lend support to the idea of Pd(II)-mediated base pairs that are highly stable but incompatible with the geometry of a double helix.

1. Introduction

The potential of metal-mediated base pairing to stabilize oligonucleotide duplexes has been demonstrated with various natural and artificial nucleobases bridged by various transition metal ions [1–9]. We are interested in harnessing this stabilization for diagnostic and therapeutic applications and to that end have studied the hybridization properties of a number of oligonucleotides incorporating an artificial organomercury or -palladium nucleobase [1,10]. These organometallic complexes resist dissociation even under dilute and metal-deficient conditions and should, hence, allow metal-mediated base pairing in biological media. Biological activity of one organopalladium oligonucleotide has already been proven in a splice-switching assay in human cell lines [11].

With organomercury nucleobases, high stability of a Hg(II)-mediated base pair at monomer level generally translates into a high UV melting temperature (T_m) of a double helix incorporating the same base pair [12,13] but with organopalladium nucleobases the situation is far less clear-cut. The 2,6-bis(3,5-dimethylpyrazol-1-yl)purine—Pd(II)—uracil base pair, for example, has an estimated dissociation constant of approximately 30 μM [14] but is still strongly destabilizing when placed in the middle of a double-helical oligonucleotide [15]. At a terminal position, however, the same base pair is strongly stabilizing, most likely owing to less strict steric constraints at the ends of a base stack than in the middle of it. This interpretation receives support from similar results on pyridine-2,6-carboxamide—Pd(II)—uracil and –thymine base pairs (Fig. 1A) [16,17] as well as the recent observation that in the middle of a double helix a flexible benzaldoxime palladacycle (Fig. 1B) is tolerated better than its rigid counterpart (Fig. 1C) [18]. The Pd(II) complexes of dipicolinic and chelidamic acid offer another interesting example of the difficulty of forming Pd(II)-mediated base pairs in the middle of a double helix. No stabilization of a duplex incorporating a central dipicolinic acid—pyridine base pair (Fig. 1D) was observed on addition of $Pd(NO_3)_2$ [19] while the monomeric Pd(II) complex of the closely related chelidamic acid readily formed an array of stacked Pd(II)-mediated base pairs with each of the adenine bases of a homoadenine oligonucleotide (Fig. 1E) [20].

In principle, even if the geometry of a metal-mediated base pair is

* Corresponding author.
E-mail address: tuanlo@utu.fi (T. Lönnberg).

[1] The contributions of Madhuri Hande and Sajal Maity should be considered equal.

https://doi.org/10.1016/j.jinorgbio.2021.111506
Received 19 April 2021; Received in revised form 18 May 2021; Accepted 30 May 2021
Available online 2 June 2021

incompatible with base stacking within a double helix, its stability may be so high that its formation is favored at the expense of neighboring Watson—Crick base pairs. In such a case, a low UV melting temperature would be observed even if complete strand dissociation would take place only at a much higher temperature. In the present paper we have explored this possibility with a competition assay between organopalladium oligonucleotides and their unmodified counterparts. Phenylpyridine palladacycle, previously studied in the middle of short double-helical oligonucleotides, was selected as the organopalladium base moiety and the sequence set was expanded to also place the putative Pd(II)-mediated base pair at either end of the duplex.

2. Results and discussion

2.1. Oligonucleotide synthesis

Table 1 summarizes the oligonucleotide sequences used in the present study. Synthesis of oligonucleotides **ON1cpc** and **ON1cpc-Pd**, bearing either an unpalladated or a palladacyclic phenylpyridine *C*-nucleoside in the middle of the sequence, has been described previously [21]. Oligonucleotides **ON1pcc** and **ON1ccp**, incorporating the same phenylpyridine residue at either 5′- or 3′-terminus, were assembled on an automated DNA/RNA synthesizer using the same phosphoramidite building block. Coupling time for this modified building block was extended to 300 s and conventional procedures were followed otherwise. In the case of the 3′-modified **ON1ccp**, the synthesis was carried out on a universal support. After chain assembly, conventional ammonolysis was used to release the oligonucleotides from the solid support

Table 1
Oligonucleotides used in this study.

Oligonucleotide	Sequence[a]
ON1pcc	5′-PGAGCCCTGGC-3′
ON1pcc-Pd	5′-P^{Pd}GAGCCCTGGC-3′
ON1cpc	5′-CGAGCPCTGGC-3′
ON1cpc-Pd	5′-CGAGCP^{Pd}CTGGC-3′
ON1ccp	5′-CGAGCCCTGGP-3′
ON1ccp-Pd	5′-CGAGCCCTGGP^{Pd}-3′
ON1cac	5′-CGAGCACTGGC-3′
ON1cac-Dabcyl	5′-CGAGCACTGGC-Dabcyl-3′
ON1ccc-Dabcyl	5′-CGAGCCCTGGC-Dabcyl-3′
ON1cgc-Dabcyl	5′-CGAGCGCTGGC-Dabcyl-3′
ON1ctc-Dabcyl	5′-CGAGCTCTGGC-Dabcyl-3′
ON2agg	5′-ACCAGGGCTCG-3′
ON2cgg	5′-CCCAGGGCTCG-3′
ON2ggg	5′-GCCAGGGCTCG-3′
ON2tgg	5′-TCCAGGGCTCG-3′
ON2gga	5′-GCCAGGGCTCA-3′
ON2ggc	5′-GCCAGGGCTCC-3′
ON2ggg	5′-GCCAGGGCTCG-3′
ON2ggt	5′-GCCAGGGCTCT-3′
ON2gag-Fam	5′-Fam-GCCAGAGCTCG-3′
ON2gcg-Fam	5′-Fam-GCCAGCGCTCG-3′
ON2ggg-Fam	5′-Fam-GCCAGGGCTCG-3′
ON2gtg-Fam	5′-Fam-GCCAGTGCTCG-3′

[a] P refers to phenylpyridine, P^{Pd} to phenylpyridine palladacycle, Dabcyl to 4-(4-dimethylaminophenyl)diazenylbenzoic acid and Fam to 6-carboxyfluorescein. In each sequence, the variable residues have been underlined.

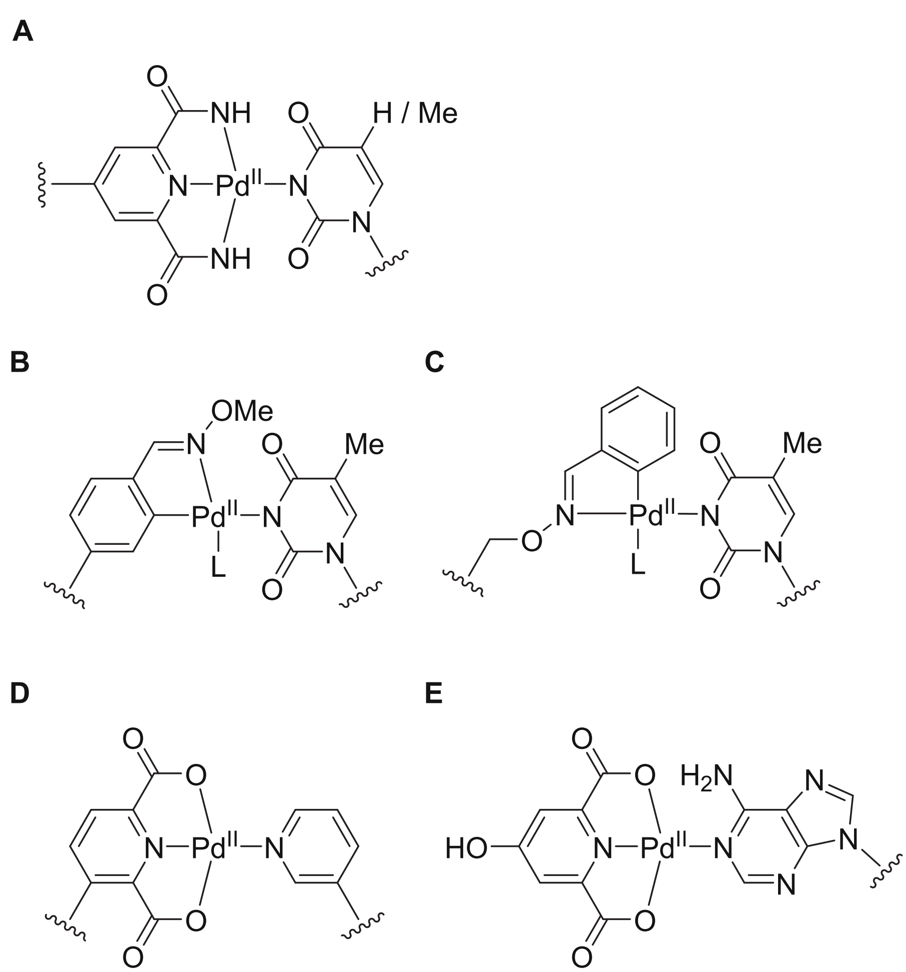

Fig. 1. Proposed Pd(II)-mediated base pairs formed by coordinative and organometallic Pd(II) complexes.

and to remove the base and phosphate protections. Finally, the phenylpyridine moieties of **ON1pcc** and **ON1ccp** were cyclopalladated by incubation in an aqueous solution of lithium tetrachloropalladate (Scheme 1). Oligonucleotides **ON1pcc** and **ON1ccp** as well as their palladacyclic counterparts **ON1pcc-Pd** and **ON1ccp-Pd** were purified by reversed-phase high-performance liquid chromatography (RP-HPLC), characterized by electrospray ionization time-of-flight mass spectrometry (ESI-TOF-MS) and quantified by UV spectrophotometry. **ON1pcc-Pd** and **ON1ccp-Pd** were, in all likelihood, initially obtained as chlorido-bridged dimers but the mass spectrometric analysis suggested that these dimers dissociate during chromatographic purification, as reported previously for related structures [18,21,22].

2.2. UV melting studies

To complement earlier studies on oligonucleotide duplexes featuring a phenylpyridine palladacycle residue in the middle of the sequence [21], hybridization properties of **ON1pcc-Pd** and **ON1ccp-Pd**, as well as their unpalladated counterparts **ON1pcc** and **ON1ccp**, were studied by conventional UV melting temperature measurements. Accordingly, the 5′-modified **ON1pcc** and **ON1pcc-Pd** were allowed to hybridize with **ON2gga**, **ON2ggc**, **ON2ggg** and **ON2ggt** and the 3′-modified **ON1ccp** and **ON1ccp-Pd** with **ON2agg**, **ON2cgg**, **ON2ggg** and **ON2tgg**, placing each of the canonical nucleobases opposite to the phenylpyridine residue. Each sample had a 1.0 μM concentration of both oligonucleotides, pH of 7.4 (20 mM cacodylate buffer) and ionic strength of 0.10 M (adjusted with sodium perchlorate). Before measurement, the samples were annealed by heating them to 90 °C and then allowing them to gradually cool down to ambient temperature.

Denaturation curves of duplexes **ON1pcc•ON2ggg**, **ON1pcc-Pd•ON2ggg**, **ON1ccp•ON2ggg** and **ON1ccp-Pd•ON2ggg** are shown in Fig. 2 as representative examples. All duplexes formed by the unpalladated oligonucleotides **ON1pcc** and **ON1cpp** exhibited monophasic sigmoidal curves typical of denaturation of a double helix. Melting curves of duplexes formed by the palladacyclic oligonucleotides **ON1pcc-Pd** and **ON1ccp-Pd**, in turn, were biphasic with an additional high-temperature transition. Furthermore, while denaturation and renaturation curves of the unpalladated duplexes were superimposable, considerable hysteresis was observed with their palladacyclic counterparts, presumably owing to relatively slow ligand exchange of Pd(II). In all cases, melting temperatures were obtained by fitting of Gaussian peaks to the first derivative curves of the UV melting profiles. This analysis, along with UV melting curves for all duplexes, is presented in the Supporting Information.

Fig. 3 summarizes the melting temperatures determined for the duplexes formed by **ON1pcc-Pd** and **ON1ccp-Pd** and their unpalladated counterparts **ON1pcc** and **ON1ccp** (numerical values can be found in the Supporting Information). With **ON1pcc**, all duplexes melted between 54 and 56 °C, similar to fully matched unmodified duplexes of the same length. Melting temperatures of the duplexes formed by **ON1ccp** were significantly lower but again similar to each other, ranging from 49 to 51 °C. In other words, replacing the 5′-terminal nucleobase with phenylpyridine had little effect on duplex stability whereas replacing the 3′-terminal nucleobase was much more detrimental. In both cases, independence of the melting temperature on the identity of the canonical nucleobase opposite to phenylpyridine suggests no specific interactions between the two.

The palladacyclic duplexes featured two melting temperatures, of which the lower one was associated with a larger thermal hyperchromicity and was, hence, interpreted as the melting temperature of the Watson—Crick base paired part of the duplex. Comparison of these values with the melting temperatures of the undpalladated duplexes revealed in most cases significant destabilization on cyclopalladation of the phenylpyridine residue. A notable exception was **ON1ccp-Pd•ON2cgg**, melting at a 5.5 °C higher temperature than **ON1ccp•ON2cgg** (T_m = 56.4 and 50.9 °C, respectively). In contrast to their unpalladated counterparts, both **ON1pcc-Pd** and **ON1ccp-Pd** exhibited very different affinities for the complementary strands depending on which canonical nucleobase was placed opposite to the phenylpyridine palladacycle. Such a dependence would be consistent with Pd(II)-mediated base pairing, while the low melting temperatures observed for most duplexes would indicate incompatibility of the geometry of the Pd(II)-mediated base pair with that of the double helix.

The denaturation curves of all palladated duplexes showed a second transition at a considerably higher temperature than the melting temperatures of the unpalladated duplexes (65—78 °C). On the renaturation curves, the two transitions merged, preventing reliable determination of the corresponding melting temperatures (data shown in the Supporting Information). A rough correlation could be observed between the higher and lower melting temperatures of the palladated duplexes. **ON1ccp-Pd•ON2cgg**, for example, exhibited the highest T_m value for both transitions (56.4 and 77.5 °C, respectively). Thermal hyperchromicities associated with the higher melting temperature were smaller than those associated with the lower melting temperature, suggesting a relatively minor change in the secondary structure of the oligonucleotides. We therefore propose that the higher-temperature transition involves dissociation of the Pd(II)-mediated base pair itself, after the rest of the duplex is already largely denatured. Unfortunately, the data at hand does not allow a meaningful proposal of the structures of the putative Pd (II)-mediated base pairs beyond what is known about Pd(II)—nucleobase coordination chemistry in general (i.e. the preference of pyrimidine N3 and purine N1 and N7 as the donor atom [23]).

2.3. Fluorescence-based competition studies

To complement the UV melting studies, the ability of the palladacyclic oligonucleotides **ON1pcc-Pd**, **ON1cpc-Pd** and **ON1ccp-Pd**, as well as their unpalladated counterparts **ON1pcc**, **ON1cpc** and **ON1ccp**, to displace an unmodified strand from a double helix was quantified by a Förster resonance energy transfer (FRET) -based competition assay. Four fully matched target duplexes were employed (**ON1ctc-Dabcyl•ON2gag-Fam**, **ON1cgc-Dabcyl•ON2gcg-Fam**, **ON1ccc-**

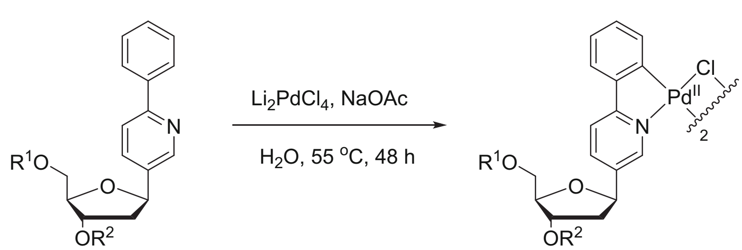

ON1pcc : R^1 = H, R^2 = 5′-GAGCCCTGGC
ON1ccp : R^1 = CGAGCCCTGG-3′, R^2 = H

ON1pcc-Pd : R^1 = H, R^2 = 5′-GAGCCCTGGC
ON1ccp-Pd : R^1 = CGAGCCCTGG-3′, R^2 = H

Scheme 1. Cyclopalladation of oligonucleotides **ON1pcc** and **ON1ccp**.

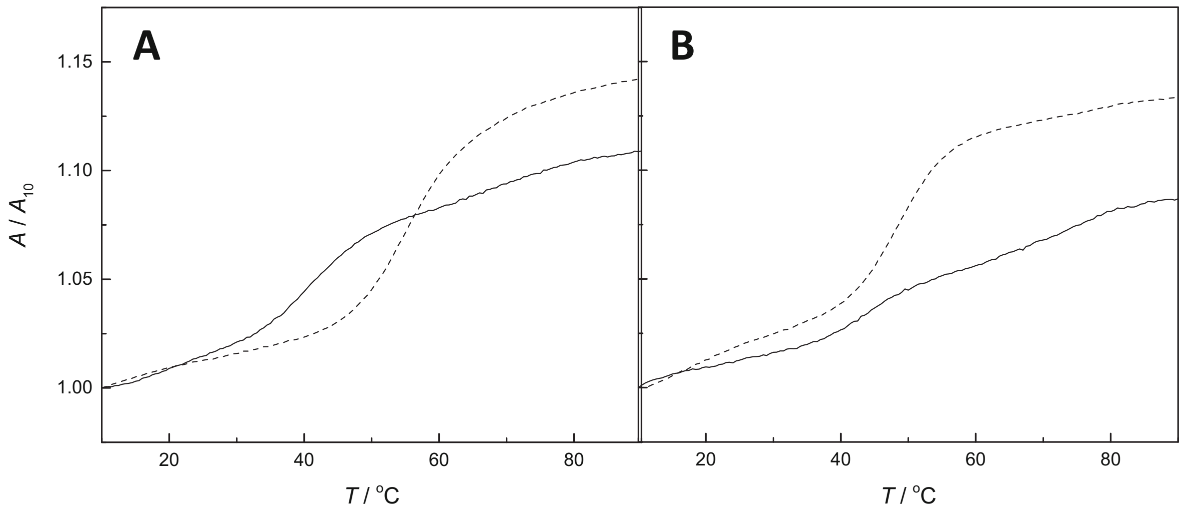

Fig. 2. UV melting profiles of duplexes A) **ON1pcc•ON2ggg** and **ON1pcc-Pd•ON2ggg** and B) **ON1ccp•ON2ggg** and **ON1ccp-Pd•ON2ggg**; pH = 7.4 (20 mM cacodylate buffer); [oligonucleotides] = 1.0 μM; $I(NaClO_4)$ = 0.10 M. In both panels, dashed line refers to the unpalladated and solid line to the palladated duplex.

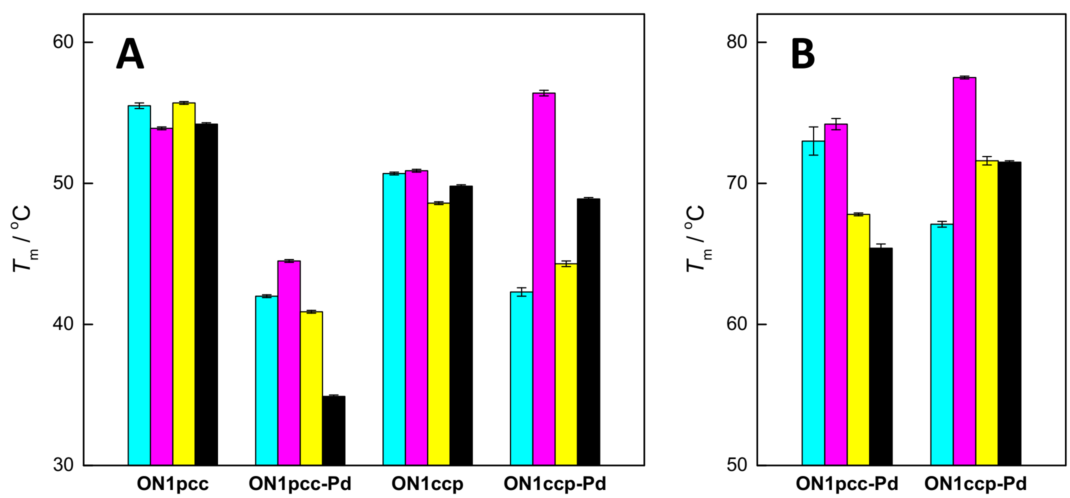

Fig. 3. A) lower and B) higher UV melting temperatures of duplexes formed by the modified oligonucleotides **ON1pcc**, **ON1pcc-Pd**, **ON1ccp** and **ON1ccp-Pd** with their natural complements **ON2gga/ON2agg** (cyan), **ON2ggc/ON2cgg** (magenta), **ON2ggg** (yellow) and **ON2ggt/ON2tgg** (black); pH = 7.4 (20 mM cacodylate buffer); [oligonucleotides] = 1.0 μM; $I(NaClO_4)$ = 0.10 M. (For interpretation of the references to colour in this figure legend, the reader is referred to the web version of this article.)

Dabcyl•ON2ggg-Fam and **ON1cac-Dabcyl•ON2gtg-Fam**), each one featuring a fluorophore (6-carboxyfluorescein, Fam) and a quencher (4-{[4-(dimethylamino)phenyl]azo}benzoic acid, Dabcyl) in close proximity at one end of the duplex. The target duplexes were designed to be only weakly emissive in their hybridized form but strongly emissive when the two strands are dissociated, either by increased temperature or competitive hybridization of a third strand. In the case of **ON1cpc-Pd**, the assay provides an independent method to study the base pairing preferences of phenylpyridine palladacycle within an oligonucleotide. With the terminally modified **ON1pcc-Pd** and **ON1ccp-Pd**, in turn, fidelity of canonical Watson—Crick base pairing away from the putative Pd(II)-mediated base pairing can be studied. Finally, comparison of the ability of the three palladacyclic oligonucleotides to displace **ON1ccc-Dabcyl** from duplex **ON1ccc-Dabcyl•ON2ggg-Fam** allows assessment of the sequence dependence of Pd(II)-mediated base pairing.

The samples used in the FRET-based competition assay were prepared otherwise identically to those used in the UV melting studies but, owing to the greater sensitivity of fluorescence, the oligonucleotide concentrations employed were only 50 nM. First, fluorescence emission spectra of the target duplexes on excitation at 493 nm were acquired at 10 and 90 °C. In both cases, a single maximum at 525 nm was observed (illustrative examples is presented in Fig. 4 and all spectra in the Supporting Information). As expected, the emission greatly increased on heating the sample from 10 to 90 °C, consistent with thermal denaturation of the double helix and dissociation of the FRET pair. The values recorded at 10 and 90 °C were taken as reference values, representing fully hybridized and dissociated states of the target duplexes, respectively.

The competition assay was first validated with the natural oligonucleotide **ON1cac**. As this oligonucleotide has exactly the same sequence as **ON1cac-Dabcyl**, one equivalent of it would be expected to displace 50% of **ON1cac-Dabcyl** from duplex **ON1cac-Dabcyl•ON2gtg-Fam** if impact of the FRET pair on duplex stability is negligible. This hypothesis was tested by mixing equimolar amounts of **ON1cac**, **ON1cac-Dabcyl** and **ON2gtg-Fam**, recording the fluorescence emission of this sample at 10 °C (Fig. 3D) and converting the value obtained into a displacement percentage by Eq. (1).

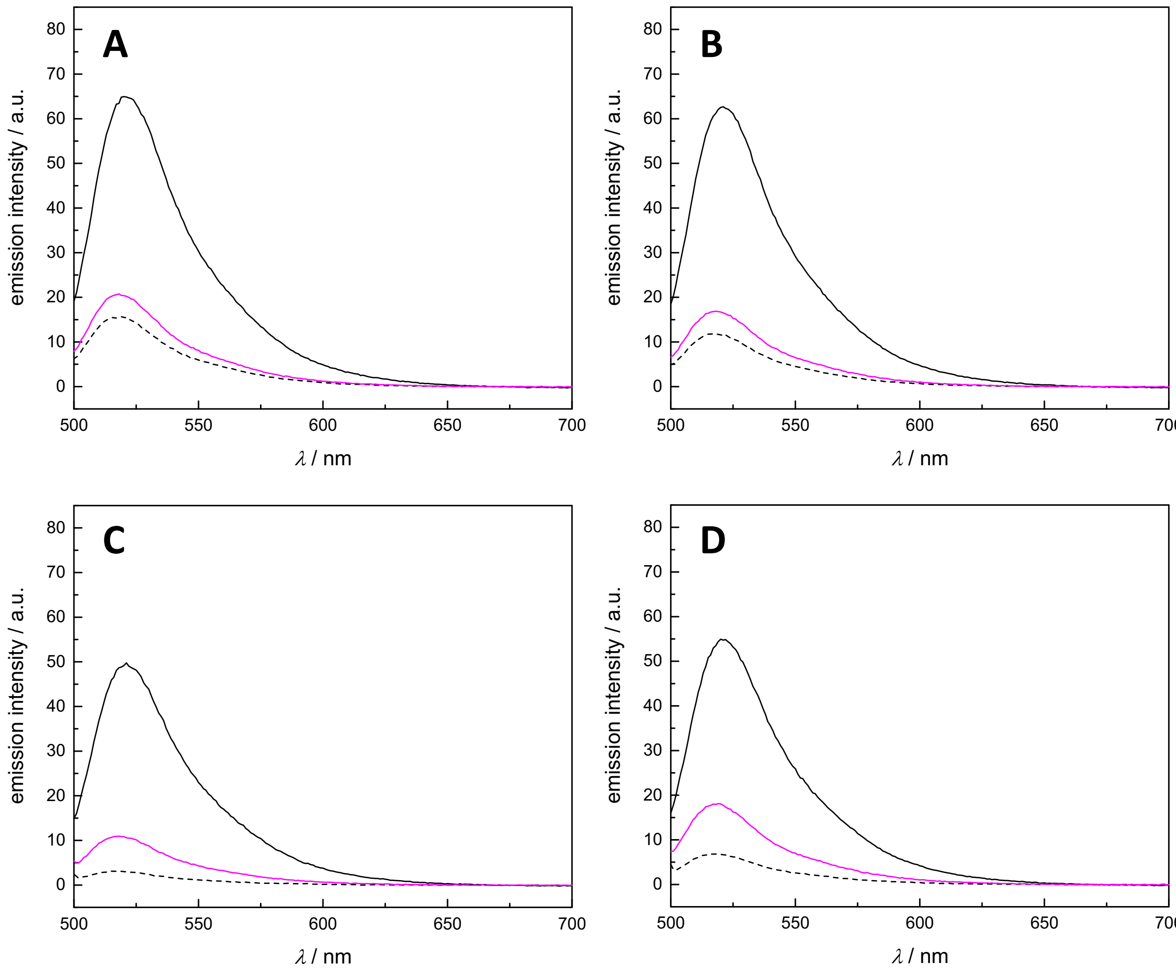

Fig. 4. Fluorescence emission spectra of duplexes **ON1ctc-Dabcyl•ON2gag-Fam** (A), **ON1cgc-Dabcyl•ON2gcg-Fam** (B), **ON1ccc-Dabcyl•ON2ggg-Fam** (C) and **ON1cac-Dabcyl•ON2gtg-Fam** (D) at 10 °C (dashed black line), 90 °C (solid black line) and at 10 °C in the presence of an equimolar amount of **ON1cac** (solid magenta line); pH = 7.4 (20 mM cacodylate buffer); [oligonucleotides] = 50 nM; $I(NaClO_4)$ = 0.10 M; λ_{ex} = 493 nm. (For interpretation of the references to colour in this figure legend, the reader is referred to the web version of this article.)

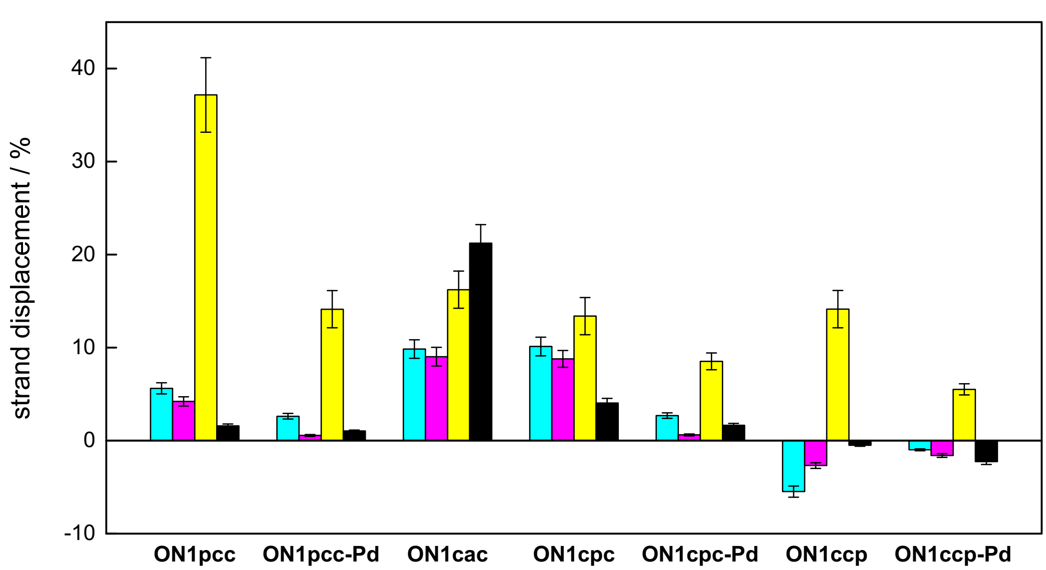

Fig. 5. Strand displacement from duplexes **ON1ctc-Dabcyl•ON2gag-Fam** (cyan), **ON1cgc-Dabcyl•ON2gcg-Fam** (magenta), **ON1ccc-Dabcyl•ON2ggg-Fam** (yellow) and **ON1cac-Dabcyl•ON2gtg-Fam** (black) by various modified and natural oligonucleotides; T = 10 °C; pH = 7.4 (20 mM cacodylate buffer); [oligonucleotides] = 50 nM; $I(NaClO_4)$ = 0.10 M. (For interpretation of the references to colour in this figure legend, the reader is referred to the web version of this article.)

$$\%displaced = \frac{intensity(mixture\,at\,10^{\circ}C) - intensity(target\,duplex\,at\,10^{\circ}C)}{intensity(target\,duplex\,at\,90^{\circ}C) - intensity(target\,duplex\,at\,10^{\circ}C)} \quad (1)$$

Curiously, the value thus obtained for **ON1cac** with **ON1cac-Dabcyl•ON2gtg-Fam** was only 21%, suggesting attractive interaction between the Fam and Dabcyl moieties. Even weaker displacement was observed with the other target duplexes (Fig. 4A–C), consistent with the presence of a single mismatch in the middle of the sequence. With this information in hand, strand displacements with all combinations of the modified oligonucleotides and target duplexes were determined in the same way and the results are summarized in Fig. 5.

ON1cpc, bearing a phenylpyridine residue opposite to the variable nucleobase within the complementary sequence, was able to displace a significant amount of the quencher strand from all of the target duplexes. The displacement percentages were comparable to those observed with the natural oligonucleotide **ON1cac** except that displacement of **ON1cac-Dabcyl** was not particularly favored. **ON1ccc-Dabcyl** was displaced somewhat more readily than the other quencher strands but overall the dependence on the canonical nucleobase opposite to phenylpyridine was modest. Cyclopalladation of the phenylpyridine moiety decreased the displacement ability with all target duplexes but considerable displacement of **ON1ccc-Dabcyl** was still observed. The phenylpyridine palladacycle, hence, appeared to favor guanine as a base pairing partner, in line with previous results of UV melting studies on **ON1cpc-Pd** [21].

ON1pcc and **ON1ccp** both favored displacement of **ON1ggg-Dabcyl**. This result was expected as in those cases the resulting duplex (**ON1pcc•ON2ggg-Fam** or **ON1ccp•ON2ggg-Fam**) has an uninterrupted stretch of 10 matched Watson—Crick base pairs whereas the other duplexes would all contain an internal mismatch. It is, however, interesting to note that with both **ON1pcc** and **ON1ccp** the strand displacement ability depended on the identity of the variable nucleobase much more strongly than with the unmodified **ON1cac**. The difference in the strand displacement ability between **ON1pcc** and **ON1ccp**, in turn, is in good agreement with the difference in the melting temperatures of duplexes formed by these oligonucleotides with their natural counterparts. As discussed above in the case **ON1cpc**, cyclopalladation of the phenylpyridine moiety was detrimental to the strand displacement ability also with **ON1pcc** and **ON1ccp**. With **ON1ccc-Dabcyl•ON2ggg-Fam** as the target duplex, strand displacement ability decreased in the order **ON1pcc-Pd** > **ON1cpc-Pd** > **ON1ccp-Pd**. In other words, the putative Pd(II)-mediated base pair between the phenylpyridine palladacycle and guanine seems to be tolerated best at the 5′-terminus and, somewhat unexpectedly, worst at the 3′-terminus. This result is in apparent conflict with those of the UV melting studies, underlining the importance of using multiple techniques when studying highly stable metal-mediated base pairs in an oligonucleotide context.

2.4. CD spectropolarimetric studies

Secondary structure of the duplexes formed by the modified oligonucleotides was studied circular dichroism (CD) spectropolarimetrically

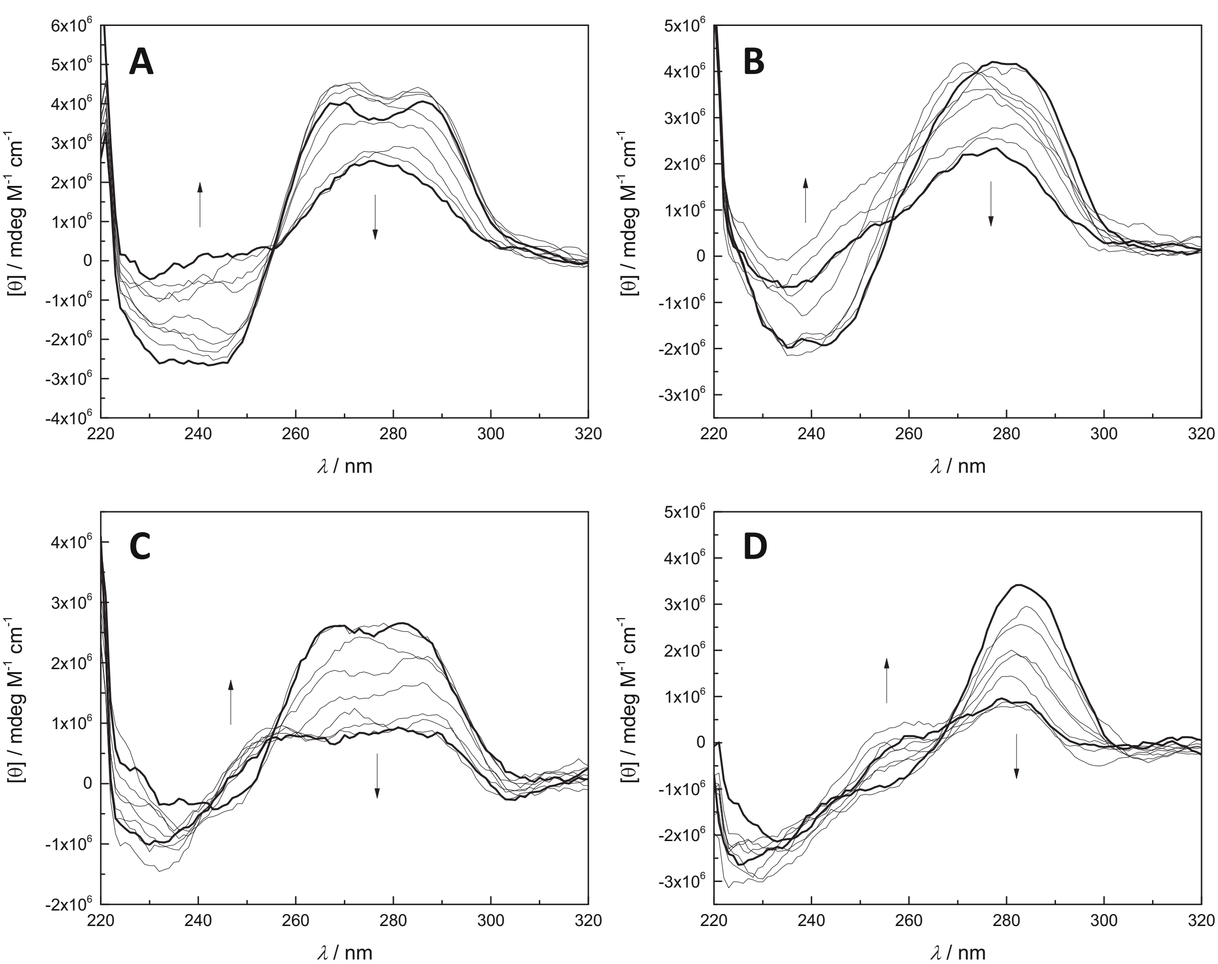

Fig. 6. CD spectra of duplexes A) **ON1pcc•ON2ggc**, B) **ON1ccp•ON2cgg**, C) **ON1pcc-Pd•ON2ggc** and D) **ON1ccp-Pd•ON2ggc**, recorded at 10 °C intervals between 10 and 90 °C; pH = 7.4 (20 mM cacodylate buffer); [oligonucleotides] = 1.0 μM; $I(NaClO_4)$ = 0.10 M. The spectra acquired at the extreme temperatures are indicated by thicker lines and the thermal loss of ellipticity by arrows.

at various temperatures covering a range of 10—90 °C. The spectra recorded for the unpalladated duplexes at 10 °C were consistent with a B-type double helical structure, with minima at 240 nm and maxima between 260 and 270 nm (illustrative examples are presented in Fig. 6 and all spectra in the Supporting Information). Curiously, a second maximum between 280 and 290 nm was observed with the duplexes formed by the 5′-modified **ON1pcc** (Fig. 6A). All minima and maxima diminished on increasing temperature, consistent with unwinding of the double helix. While spectra of the palladacyclic duplexes at 10 °C were also mostly characteristic of right-handed double helices, notable differences compared to the spectra of the unpalladated duplexes could also be detected. The minima at 240 nm were less pronounced or even nonexistent and in the spectrum of **ON1ccp-Pd•ON2ggg** also the maximum was very weak. Thermal diminution of the minima and maxima was observed also with the palladacyclic duplexes but, in contrast to the unpalladated duplexes, in many cases a new maximum appeared at 250 nm.

Unfortunately, in most cases the CD data was too scattered to allow reliable determination of CD melting temperatures. For some duplexes, however, a reasonable approximation could be obtained as the inflection point of a dose-response curve fitted to temperature-dependent molar ellipticity at 280 nm (illustrative examples are presented in Fig. 7). With the palladacyclic duplexes **ON1pcc-Pd•ON2ggc** and **ON1ccp-Pd•ON2cgg**, the values thus obtained were in reasonable agreement with the lower UV melting temperatures (46 ± 3 vs. 44.5 ± 0.1 °C and 52 ± 6 vs. 56.4 ± 0.2 °C, respectively). With the unpalladated counterparts **ON1pcc•ON2ggc** and **ON1ccp•ON2cgg**, on the other hand, the correlation was much less clear (65 ± 3 vs. 53.9 ± 0.1 °C and 72 ± 3 vs. 50.9 ± 0.1 °C, respectively). The higher UV melting temperature of the palladacyclic duplexes could not be reproduced based on the CD data, presumably owing to the small hyperchromicity of the related transition. It seems clear, however, that the phenylpyridine palladacycle distorts the double helix and that the effect is much more pronounced at the 3′-terminus than at the 5′-terminus.

3. Conclusions

With few exceptions, oligonucleotide duplexes incorporating a phenylpyridine palladacycle at either 5′- or 3′-terminus were found to be less stable than their unpalladated counterparts. The results obtained by UV melting and FRET-based competition studies were not in complete agreement, however, and a small additional high-temperature transition in the UV melting profiles of the palladated duplexes would seem to suggest that Pd(II)-mediated base pairs between the phenylpyridine palladacycle and canonical nucleobases persist at temperatures exceeding the melting temperature of the Watson—Crick part of the duplex.

4. Experimental

4.1. General methods

Commercially available reagents, including the Dabcyl- and FAM-labeled oligonucleotides, were used as received. The sole exception was triethylamine, which was distilled before preparation of the HPLC elution buffer. Mass spectra were recorded on a Bruker Daltonics micrOTOF-Q mass spectrometer.

4.2. Oligonucleotide synthesis

Synthesis of the phenylpyridine-modified oligonucleotide **ON1cpc** and its palladacyclic derivative **ON1cpc-Pd** has been described previously [21]. The corresponding terminally modified oligonucleotides **ON1pcc** and **ON1ccp** were assembled on an Applied Biosystems 3400 automated DNA/RNA synthesizer using the same building block for introduction of the phenylpyridine *C*-nucleoside. Standard phosphoramidite strategy was followed except that the coupling time for the phenylpyridine *C*-nucleoside building block was extended to 300 s. Normal coupling yields were observed throughout the sequence by trityl release monitoring. On completion of chain assembly, oligonucleotides **ON1pcc** and **ON1ccp** were deprotected and released from the solid support by incubation in 25% aqueous ammonia at 55 °C for 16 h. The crude oligonucleotides were purified by RP-HPLC on a Hypersil ODS C18 column (250 × 4.6 mm, 5 μm) eluting with a linear gradient (5—30% over 30 min, 1 mL min^{-1}) of acetonitrile in 50 mM aqueous triethylammonium acetate, the detection wavelength being 260 nm. Pure oligonucleotides **ON1pcc** and **ON1ccp** were characterized by ESI-TOF-MS and quantified by UV spectrophotometry.

Cyclopalladtion of **ON1pcc** and **ON1ccp** was carried out by incubation of these oligonucleotides (34.58 and 32.26 nmol, respectively), Li_2PdCl_4 (5 nmol) and NaOAc (20 nmol) in H2O (10 μL) at 55 °C for 24 h. The product mixtures were fractioned by RP-HPLC on a Hypersil ODS C18 column (250 × 4.6 mm, 5 μm) eluting with a linear gradient (5—30% over 30 min, 1 mL min^{-1}) of acetonitrile in 50 mM aqueous triethylammonium acetate, the detection wavelength being 260 nm. Pure oligonucleotides **ON1pcc-Pd** and **ON1ccp-Pd** thus obtained were characterized by ESI-TOF-MS and quantified by UV spectrophotometry.

4.3. UV melting experiments

UV melting curves were acquired on a PerkinElmer Lambda 35 UV–vis spectrophotometer equipped with a Peltier temperature control unit. The samples were prepared in quartz glass cuvettes of 10.00 mm optical path by mixing the appropriate oligonucleotides to a final concentration of 1.0 μM. The pH of the samples was adjusted to 7.4 with 20 mM cacodylate buffer and the ionic strength to 0.10 M with $NaClO_4$.

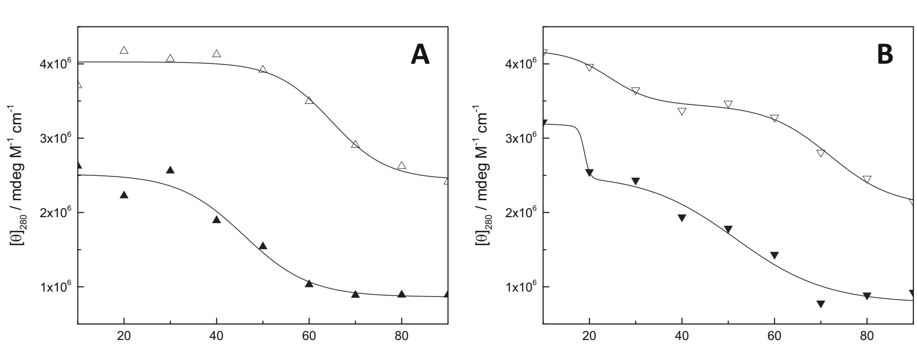

Fig. 7. Molar ellipticity at 280 nm as a function of temperature for duplexes A) **ON1pcc•ON2ggc** (△) and **ON1pcc-Pd•ON2ggc** (▲) and B) **ON1ccp•ON2cgg** (▽) and **ON1ccp-Pd•ON2ggc** (▼); pH = 7.4 (20 mM cacodylate buffer); [oligonucleotides] = 1.0 μM; *I*($NaClO_4$) = 0.10 M. The lines are dose-response curves fitted to the experimental data points.

Before measurement, the samples were annealed by heating to 90 °C followed by gradual cooling to ambient temperature. Each sample was subjected to three heating and cooling ramps (10—90 °C, 0.5 °C min^{-1}) and absorbance at 260 nm was recorded at 0.5 °C intervals. The melting temperatures were determined as the center points of Gaussian peaks fitted to the first derivative curves of the UV melting profiles.

4.4. FRET-based competition experiments

Fluorescence emission spectra were acquired on a Cary Eclipse fluorescence spectrometer over a range of 500—700 nm, the excitation wavelength being 493 nm. The excitation and emission slits were set to 5 nm, the PMT voltage to 600 V and the scan rate to 120 nm min^{-1}. The samples were prepared in otherwise the same way as in the UV melting studies except that the oligonucleotide concentration was reduced to 50 nM. Each of the target duplexes (**ON1ctc-Dabcyl•ON2gag-Fam**, **ON1cgc-Dabcyl•ON2gcg-Fam**, **ON1ccc-Dabcyl•ON2ggg-Fam** and **ON1cac-Dabcyl•ON2gtg-Fam**) was first annealed by heating to 90 °C and then gradually cooling down to 10 °C, after which the emission spectra were recorded at 10 and 90 °C. The duplex samples were then split to seven parts and an equimolar amount of one of the displacer oligonucleotides (**ON1pcc**, **ON1pcc-Pd**, **ON1cac**, **ON1cpc**, **ON1cpc-Pd**, **ON1ccp** and **ON1ccp-Pd**) was added to each. The resulting samples were then again heated to 90 °C and cooled gradually to 10 °C, at which temperature emission spectra were recorded.

4.5. CD experiments

CD spectra were acquired on an Applied Photophysics Chirascan spectropolarimeter equipped with a Peltier temperature control unit. Samples and cuvettes were identical to those used in the UV melting experiments. Nine spectra at 10 °C intervals, covering a temperature range of 10—90 °C were recorded for each sample. The samples were allowed to equilibrate at the measurement temperature for either 120 s (unmetallated duplexes) or 1800 s (metallated duplexes) before acquisition of the spectrum. The wavelength range was limited to 220—320 nm as no Cotton effects were observed outside this range.

Declaration of Competing Interest

The authors have no competing interests to declare.

Acknowledgements

This project has received funding from the European Union's Horizon 2020 research and innovation programme under the Marie Skłodowska-Curie grant agreement no 721613, from the Academy of Finland (decisions 286478 and 294008) and Turku University Foundation (decision 080803).

Appendix A. Supplementary data

Supplementary data to this article can be found online at https://doi.org/10.1016/j.jinorgbio.2021.111506.

References

[1] D. Ukale, T. Lönnberg, ChemBioChem 22 (2021) 1733–1739, cbic.202000821.
[2] S. Naskar, R. Guha, J. Müller, Angew. Chem. Int. Ed. 59 (2020) 1397–1406.
[3] B. Jash, J. Müller, Chem. Eur. J. 23 (2017) 17166–17178.
[4] Y. Takezawa, J. Müller, M. Shionoya, Chem. Lett. 46 (2017) 622–633.
[5] B. Lippert, P.J. Sanz Miguel, Acc. Chem. Res. 49 (2016) 1537–1545.
[6] S. Taherpour, O. Golubev, T. Lönnberg, Inorg. Chim. Acta 452 (2016) 43–49.
[7] P. Scharf, J. Müller, ChemPlusChem 78 (2013) 20–34.
[8] Y. Takezawa, M. Shionoya, Acc. Chem. Res. 45 (2012) 2066–2076.
[9] G.H. Clever, M. Shionoya, Coord. Chem. Rev. 254 (2010) 2391–2402.
[10] D. Ukale, S. Maity, M. Hande, T. Lönnberg, Synlett 30 (2019) 1733–1737.
[11] M. Hande, O. Saher, K.E. Lundin, C.I.E. Smith, R. Zain, T. Lönnberg, Molecules 24 (2019) 1180.
[12] D. Ukale, V.S. Shinde, T. Lönnberg, Chem. Eur. J. 22 (2016) 7917–7923.
[13] D.U. Ukale, T. Lönnberg, Angew. Chem. Int. Ed. 57 (2018) 16171–16175.
[14] S. Taherpour, T. Lönnberg, J. Nucleic Acids 2012 (2012) 11.
[15] S. Taherpour, H. Lönnberg, T. Lönnberg, Org. Biomol. Chem. 11 (2013) 991–1000.
[16] O. Golubev, T. Lönnberg, H. Lönnberg, J. Inorg. Biochem. 139 (2014) 21–29.
[17] O. Golubev, G. Turc, T. Lönnberg, J. Inorg. Biochem. 155 (2016) 36–43.
[18] S.K. Maity, M.A. Hande, T. Lönnberg, ChemBioChem 21 (2020) 2321–2328.
[19] E. Meggers, P.L. Holland, W.B. Tolman, F.E. Romesberg, P.G. Schultz, J. Am. Chem. Soc. 122 (2000) 10714–10715.
[20] A. Pérez-Romero, A. Domínguez-Martín, S. Galli, N. Santamaría-Díaz, O. Palacios, J.A. Dobado, M. Nyman, M.A. Galindo, Angew. Chem. Int. Ed. 60 (2021) 10089–10094, anie.202015554.
[21] S.K. Maity, T. Lönnberg, Chem. Eur. J. 24 (2018) 1274–1277.
[22] M. Hande, S. Maity, T. Lönnberg, Int. J. Mol. Sci. 19 (2018) 1588.
[23] R.B. Martin, Acc. Chem. Res. 18 (1985) 32–38.